Published in final edited form as:
Arterioscler Thromb Vasc Biol. 2011 November ; 31(11): 2526–2533. doi:10.1161/ATVBAHA.111.230177.

DYSREGULATED SELECTIN EXPRESSION AND MONOCYTE RECRUITMENT DURING ISCHEMIA-RELATED VASCULAR REMODELING IN DIABETES MELLITUS

Chad L. Carr, M.D., **Yue Qi, M.D.**, **Brian Davidson, M.D.**, **Scott Chadderdon, M.D.**, **Ananda R. Jayaweera, Ph.D.**, **J. Todd Belcik, B.S., R.D.C.S.**, **Cameron Benner**, **Aris Xie, B.S.**, and **Jonathan R. Lindner, M.D.**
Division of Cardiovascular Medicine, Oregon Health & Science University, Portland, OR

Abstract

Objective—Diabetes mellitus (DM) is associated with impaired ischemia-related vascular remodeling and also dysregulation of the inflammatory response. We sought to determine whether impaired selectin-mediated monocyte recruitment in ischemic tissues contributes to blunted ischemia-mediated angiogenesis in DM.

Methods and Results—Contrast-enhanced ultrasound (CEU) perfusion imaging and molecular imaging of endothelial P-selectin expression in the proximal hindlimb were performed at 1,3, and 21 days after arterial ligation in wild-type and db/db mice. Ligation reduced muscle blood flow to ≈0.05 ml/min/g in both strains. Significant recovery of flow occurred only in wild-type mice (60–65% of baseline flow). On molecular imaging in db/db mice, baseline P-selectin signal was 4-fold higher in db/db compared to wild-type mice ($p<0.01$) but increased minimally in at day one after ischemia whereas signal increased approximately 10-fold in wild-type mice ($p<0.01$). Immunohistology of the hindlimb demonstrated severely reduced monocyte recruitment in db/db mice compared to wild-type mice. Local treatment with monocyte chemotactic protein-1 (MCP-1) corrected the deficits in post-ischemic P-selectin expression and monocyte recruitment in db/d mice, and led to greater recovery in blood flow.

Conclusions—In DM, there is dysregulation of the selectin response to limb ischemia which leads to impaired monocyte recruitment, which may be mechanistically related to reduced vascular remodeling in limb ischemia.

Keywords

Angiogenesis; Diabetes; Inflammation; Molecular Imaging; Monocytes

Growth and remodeling of collateral vessels and the distal microcirculation are important adaptations to ischemia produced by peripheral and coronary artery disease. This compensatory response is impaired in type 2 diabetes mellitus (DM).[1–3] A potential explanation is that despite smoldering chronic inflammation in DM there may be an inability to further mount a response from beneficial pro-angiogenic components of the inflammatory response.

Address correspondence to: Jonathan R. Lindner, MD, Cardiovascular Division, UHN-62, Oregon Health & Science University, 3181 SW Sam Jackson Park Rd. Portland, OR 97239, Tel. (503) 494-8750, Fax (503) 494-8550, lindnerj@ohsu.edu.

DISCLOSURES
No disclosures for any of the authors.

Certain monocyte subtypes play an important role in coordinating vascular remodeling through their production of growth factors, cytokines, and matrix proteases.[4–6] Monocyte entry into ischemic tissue is regulated by many factors including chemokines, such as monocyte chemotactic protein-1 (MCP-1), and VEGF-A. Monocytes from patients with DM exhibit a severe deficit in chemotaxis specifically to VEGF-A.[7] This deficit appears to be due to "desensitization" of monocyte VEGF-receptor (VEGFR)-1 signaling.[7–9] Yet, major gaps remain in our understanding of how a dysregulated monocyte response contributes to poor vascular remodeling in DM, including whether there is a similar desensitization of endothelial activation. Of particular interest is endothelial P-selectin expression since translocation of the P-selectin to the cell surface is stimulated by VEGF-receptor activation,[10] and some studies have indicated that recruitment of monocytes through P-selectin plays an important role in ischemia-mediated vascular remodeling.[11]

The aim of this study was to determine whether the selectin response to ischemia is abnormal in DM, and whether this leads to impairment in monocyte recruitment, arteriogenesis, and blood flow recovery. To test this hypothesis, *in vivo* contrast-enhanced ultrasound (CEU) molecular imaging of endothelial P-selectin expression was temporally correlated to quantitative muscle blood flow (MBF) measurements in a chronic ischemic hindlimb model in obese insulin-resistant (db/db) mice. We also sought to determine whether local treatment with monoycte chemotactic protein-1 (MCP-1) could compensate for deficiencies in monocyte recruitment and improve blood flow recovery in DM since it is a VEGF-independent monocyte chemokine that also promotes endothelial P-selectin translocation.[12]

METHODS

Hindlimb Ischemia Protocol

The study was approved by the Animal Care and Use Committee at Oregon Health & Science University. Hindlimb ischemia was produced by unilateral interruption of arterial inflow in 40 wild type C57Bl/6 mice and 50 db/db mice (B6.Cq-m+/+ Lepr^{db}/J, Jackson Laboratories) with a homozygous deletion of the leptin receptor that produces age-dependant obesity and insulin resistance.[13] Mice (age 8–10 weeks) were anesthetized with inhaled isoflurane (1.0–1.5%) and euthermia was maintained with a heating pad. Using sterile technique, the distal common iliac artery and the origin of the epigastric artery were ligated through a midline abdominal incision. In 6 of the wild-type mice, P-selectin functionally inhibited for approximately for approximately the first week by IP injection of rat anti-mouse P-selectin mAb (RB40.34) immediately prior to ligation.[14] In 18 of the db/db mice, MCP-1 (1 μg/kg in 50 μl) was injected intramuscularly into the proximal hindlimb adductor group of the ischemic limb immediately after ligation and on days 1 and 3 after ligation. Imaging studies were performed on days 1, 3 and 21 after ligation; and only two separate time points were used per subject which was randomly selected. For imaging mice were anesthetized and the jugular vein was catheterized for administration of contrast agent. Perfusion and molecular imaging studies were performed at baseline prior to ligation in an additional 6 wild-type and 12 db/db mice.

Microbubble Preparation

Non-targeted lipid-shelled decafluorobutane microbubbles were prepared by sonication of a gas-saturated aqueous suspension of 2 mg/mL distearoylphosphatidylcholine and 1 mg/mL of polyoxyethylene-40-stearate. For molecular imaging, biotinylated microbubbles were prepared by adding 0.4 mg/mL distearoylphosphatidylethanolamine-PEG(2000). Biotinylated rat anti-mouse P-Selectin monoclonal antibody (RB40.34) was conjugated to

the microbubble surface via a streptavidin linkage as previously described.[15] Microbubble concentration was measured by electrozone sensing (Multisizer III, Beckman Coulter).

Perfusion Imaging

Contrast ultrasound perfusion imaging was performed in the ischemic and contralateral control limb with a linear-array transducer at a centerline frequency of 7 MHz (Sequoia 512, Siemens Medical Systems). The non-linear fundamental signal component for microbubbles was detected using multipulse phase- and amplitude-modulation at a mechanical index (MI) of 0.18 and a dynamic range of 55 db. With these settings, the beam elevational plane, defined as >100 KPa peak negative acoustic pressure, is approximately 2 mm.[16] Blood pool signal (I_B) was measured from a region-of-interest placed in the left ventricular cavity at end-diastole during a microbubble intravenous infusion rate of 1×10^6 min^{-1}. The infusion rate was then increased to 1×10^7 min^{-1} for muscle imaging. The proximal hind-limb adductor muscles were imaged in a transverse plane halfway between the inguinal fold and the knee. Images were acquired at a frame rate of 20 Hz immediately after a brief high-power (MI 1.1) destructive pulse sequence and time-intensity data were fit to the function:

$$y=A(1-e^{-\beta t})$$

where *y* is intensity at time *t*, *A* is the plateau intensity, and the rate constant β represents the microvascular flux rate.[17,18] Skeletal muscle microvascular blood volume (MBV) was quantified by:

$$A/(1.06\times I_B\times F\times 1.1)$$

where 1.06 is tissue density (g/cm^3), *F* is the scaling factor for the 10-fold lower microbubble infusion rate for measuring I_B which was used to avoid dynamic range saturation, and 1.1 is a coefficient to correct for murine sternal attenuation measured *a priori* from in vitro experiments (see on-line appendix). MBF was quantified by the product of MBV and β.

Molecular Imaging

For molecular imaging, 1×10^7 P-selectin-targeted and control microbubbles were injected as an intravenous bolus in random order separated by 10–12 min. A mathematical algorithm was developed to calculate the retention fraction of microbubbles rather than simply measuring signal from retained microbubbles since this latter value is influenced by the amount of flow in the ischemic limb (i.e. the total number of bubbles fluxing through the imaging plane) which varied over time. Using low-MI imaging, ultrasound frames were acquired every 10 seconds after injection for a total of 8 min. The retention fraction (*f*) of the bubbles was calculated by fitting time-intensity data from a region-of-interest placed over the proximal hindlimb adductor muscles to the function:

$$I_T=(K\cdot A_n\cdot A)\cdot(t\cdot e^{-\alpha t}+(f\cdot\beta/\alpha^2)\cdot(1-(1+\alpha t)\cdot e^{-\alpha t}))$$

This derivation of this formula relies on the deconvolution of the time-intensity curve into two separate functions: (1) a γ-variate function reflecting freely transiting microbubbles, and (2) an integral of a γ-variate that represents retained microbubbles (see on-line Appendix). This method was ideally suited to our ischemia-angiogenesis model since *f* is independent of both tissue blood flow and microbubble dose.

Platelet Depletion

In order to determine whether the primary source of P-selectin signal was endothelial or platelet-derived, imaging was performed after immune-mediated platelet depletion in an additional 6 wild-type mice. Immediately after ligation surgery and wound closure, mice were treated with 2μg/g rat anti-mouse glycoprotein-Ibα mAb (R300, Emfret Analytics) by intraperitoneal route. This treatment has been shown to reduce platelet concentration to <10,000 dL^{-1} for >48 hrs through splenic sequestration.[19] Molecular and perfusion imaging were performed 1 day after ligation.

Echocardiography and Hemodynamic Measurements

Echocardiography (Vevo-770, Visualsonics Inc.) and invasive aortic micromanometry (SPR–671; Millar Instruments, Inc.) were performed to exclude significant strain-related differences in hemodynamics and left ventricular function under anesthesia (see online supplement for methods).

Intravital Microscopy

Selectin-mediated leukocyte rolling in post-capillary venules was assessed by intravital microscopy. Wild-type (n=6) and db/db (n=6) mice were anesthetized with an intraperitoneal injection of ketamine hydrochloride, xylazine and atropine. A cremaster muscle was exteriorized and mounted on a custom stage for intravital microscopy. The muscle was superfused continuously with isothermic bicarbonate-buffered saline during microscopy (Axioskop2-FS, Carl Zeiss, Inc., Thornwood, New York) with a saline-immersion objective (×20/0.5 N.A.). Video recordings of at least 5 venules (diameter 20–40 μm) were made with a high-resolution CCD camera (C2400, Hamamatsu Photonics, Hamamatsu, Japan) 10–20 min after exteriorization. Centerline RBC velocity (V_b) was measured using a dual-slit photodiode (CircuSoft Instrumentation) and converted to mean velocities by multiplying by 0.625. Venular diameters (d) were measured off-line using video calipers. The distance traveled by individual rolling leukocytes was divided by the elapsed time to derive the mean rolling velocity. The number of rolling leukocytes (r_n) was determined by counting leukocytes crossing a line perpendicular to the vessel during 1 min. Leukocyte rolling flux fraction, which reflects the percent of leukocytes passing through a venule that are rolling, was calculated by:

$$r_n/(0.25\pi d^2 \cdot V_b \cdot 60 \cdot C_L)$$

where C_L is the systemic blood leukocyte concentration.

Immunohistochemistry

Histology was performed with perfusion-fixed paraffin-embedded sections. Immunohistochemistry was performed for monocytes/macrophages with a rat anti-mouse Mac-2 monoclonal antibody (M3/38, Cedarlane Labs) with an ALEXA Fluor-488-labeled secondary antibody (Invitrogen). The spatial extent of positive staining was quantified by a pixel intensity threshold program (NIH Image-J) and expressed as a percent of the total muscle area per section. Non-capillary microvascular density was assessed by immunohistochemistry with a Cy3-labeled rat anti-mouse α-smooth muscle actin mAb (1A4, Sigma) and was expressed by the total microvessel area per muscle section area.

Statistics

Data are represented as mean ± standard deviation unless otherwise specified. Targeted imaging and intravital microscopy data were analyzed with non-parametric tests (Kruskal-

Wallis and Mann-Whitney test). Group comparisons for perfusion and histology were made with one-way ANOVA and post-hoc testing of individual comparisons with paired t-test and Bonferroni correction.

RESULTS

Strain-related Characteristics at Baseline

At baseline, db/db mice had a higher body mass (44±5 vs 22±5 g, $p<0.001$) and were hyperglycemic (blood glucose 443±71 vs 114±32 mg/dL, $p<0.001$) compared to wild-type mice consistent with the expected obese insulin-resistant phenotype. There were no species-related differences in blood leukocyte, erythrocyte, or platelet concentration (data not shown). Heart rate and central aortic blood pressure were similar between wild-type and db/db mice, as were echocardiographic measurements of left ventricular function such as thickening fraction, Vcf, and endocardial peak systolic radial velocity (see online supplement).

Skeletal Muscle Blood Flow

Microvascular blood flow in the proximal hindlimb adductor muscle group on CEU imaging at baseline prior to ligation was lower in db/db mice (Figure 1A). Lower baseline flow in db/db mice was due to slower microvascular blood flux rate and lower microvascular blood volume (see online supplement). On day 1 after arterial ligation, blood flow was reduced to a similar level (≈0.05 ml/min/g) for both wild-type and db/db mice (Figure 1A). Qualitatively at this time point there was considerable spatial heterogeneity in flow distribution with interspersed areas of hypoperfusion and non-perfusion within the muscle. In wild-type mice, blood flow in the ischemic muscle increased over 21 days, ultimately reaching an average of around 65% of baseline flow whereas flow recovery was minimal in db/db mice. Recovery of flow in the wild-type mice was manifest by significant increases in both microvascular blood volume and flux rate (see online supplement). On immunohistochemistry at day 21, the area of α-smooth muscle actin vessels in muscle from the ischemic limb, expressed as a ratio to the contralateral normal limb, was greater in wild-type vs. db/db mice (2.1±0.1 vs. 1.2±0.1, $p<0.01$), consistent with a substantial arteriogenic response only in wild-type mice. The degree of flow recovery at day 21 in wild-type mice varied considerably (range: 0.15 to 0.73 mL/min/g) and was inversely but nonlinearly related to the severity of initial ischemia on day 1 (Figure 1D), suggesting that the degree of initial ischemia may influence the rate of flow recovery over the first three weeks in wild-type mice. Recovery of blood flow at day 21 in wild-type mice was substantially inhibited by treatment with an antibody that functionally inhibits P-selectin, and in db/db mice was significantly augmented when treated with MCP-1 (Figure 2).

Molecular Imaging of P-selectin

At baseline prior to arterial ligation, the retention fraction for P-selectin-targeted microubbbles on molecular imaging was approximately 4-fold greater in db/db compared to wild-type mice (Figure 3A). However, in wild-type mice P-selectin signal markedly increased in wild-type mice at day 1 and 3 after ligation (10-fold and 3-fold increase from baseline, respectively) indicating an early and robust P-selectin response to ischemia in wild type animals. In db/db mice, despite having high baseline P-selectin expression, further upregulation of P-selectin in response to ischemia was severely blunted compared to wild-type mice. In db/db/ mice, treatment with MCP-1 produced a substantial increase in P-selectin signal at day 1 to a level similar to that seen in wild-type mice. Immune-mediated platelet depletion with anti-GP1bα antibody in wild-type mice was confirmed by bleeding times of >21 min. In these mice, the P-selectin signal was similar to those not undergoing platelet depletion (0.36±0.12 vs 0.36±0.22, $p=0.94$), indicating a predominantly endothelial

rather than platelet source for P-selectin signal on molecular imaging. In wild-type mice undergoing imaging at both Days 1 and 21 (n=11), there was a modest linear relationship between P-selectin signal at day 1 and flow recovery at day 21 (Figure 3B).

Intravital Microscopy

Intravital microscopy of the cremaster muscle was used as a complementary method for evaluating P-selectin mobilization to the endothelial luminal surface. In db/db mice, leukocyte mean rolling velocity was faster and leukocyte rolling flux fraction was lower in post-capillary venules observed 10–30 min after surgical exteriorization (Figure 4), consistent with an impairment in P-selectin response.

Histology

On H&E staining, there was a robust inflammatory cell infiltrate in the ischemic muscle from wild-type mice which was most pronounced at day 3 (Figure 5). On Mac-2 staining, much of the cellular infiltrate at this time interval appeared to be of monocyte origin. In db/db mice, fewer inflammatory cells were seen on H&E and the number of Mac-2-positive monocytes was markedly reduced particularly at day 3 after ligation. Treatment with MCP-1 in the early ischemic period in db/db mice resulted in an increase in total inflammatory cell infiltration and monocyte accumulation on days 1 and 3 after ligation.

DISCUSSION

The primary aim of this study was to pair molecular imaging and perfusion imaging data in a murine model of limb ischemia to determine whether impaired flow recovery in DM is associated with abnormalities in endothelial selectin expression and monocyte recruitment. Our studies demonstrated that: (1) flow recovery in response to hindlimb ischemia is severely impaired in db/db mice; (2) despite a chronic upregulation of P-selectin, further upregulation in response to ischemia is severely blunted in db/db mice; (3) monocyte recruitment, arteriogenesis, and recovery of limb perfusion are associated with and possibly influenced by the P-selectin response during ischemia; and (4) the deficits in endothelial selectin upregulation and monocyte recruitment during ischemia in db/db mice can be corrected by local treatment with MCP-1 which may explain its effect on enhancing flow recovery in these animals.

Clinical trials and animal models of disease have established that compensatory vascular remodeling in chronically ischemic tissue is abnormal in diabetic subjects.[1–3,9] Hence, the blunted recovery of limb perfusion after iliac ligation in db/db mice in the current study was expected. The severity of this abnormality was striking and somewhat greater than some prior studies that have used laser Doppler velocimetry as a surrogate for quantitative flow measurement.[9,20–23] One reason for this discrepancy is technical in nature since this is the first study that quantifies microvascular perfusion in ml/min/g of tissue and is not influenced by signal from large vessel flow. Another reason is that muscle blood flow was significantly reduced at baseline in db/db mice compared to wild-type mice, similar to what has also been found with CEU in Zucker obese rats.[24] This finding suggests that comparisons to a contralateral control limb may not reflect the true severity of flow impairment in DM.

Prior studies using histology have been consistent in finding less angiogenesis, arteriogenesis, collateral development after interruption of arterial inflow when compared to control mice.[20–23] We found that impaired flow recovery after arterial ligation in db/db mice was manifest in part by the lack of a time-dependent increase in microvascular blood volume on CEU. However, lower *functional* microvascular density derived from CEU time-intensity data does not necessarily imply a lower *anatomic* capillary density. In coronary and

peripheral arterial disease, functional capillary blood volume in vascular beds is influenced by the degree of pressure loss caused by stenosis.[25] Similar to other studies,[22,23] histology in the ischemic limb in db/db mice in our study showed less arteriogenesis, which would be expected to lead to lower collateral conductance in the ischemic limb, lower pre-capillary pressure, and subsequent capillary derecruitment.[25] The fact that microvascular blood flux rate was equally impaired suggests that this was the case.

There is strong evidence that monocytes play a critical role in arteriogenesis and other vascular responses to tissue ischemia and injury. In mammalian models of limb ischemia, potentiation of the monocyte response with chemokines such as MCP-1 and LPS have been shown to augment collateral development.[6,26] Mice that are deficient in either MCP-1 or CCR-2, a primary receptor for MCP-1, have less recovery of limb blood flow after interruption of the arterial inflow supply.[27,28] These findings are thought to be related to the finding of less perivascular monocyte infiltration since these cells are thought to contribute to vascular remodeling through production of growth factors (VEGFs, FGF-2, PDGF, PlGF, HIF-1α, etc), pro-angiogenic cytokines, and matrix proteases. In the current study, db/db mice had a striking reduction in the extent of monocyte infiltration early after producing ischemia. Impaired VEGF-A-mediated monocyte migration may have contributed to this abnormality.[7,8] However, our results also suggest that abnormalities in the initial step of selectin-mediated monocyte recruitment may have also contributed. The idea to study selectins in this setting was based on their recognized role in monocyte recruitment and angiogenesis in limb ischemia and wound healing,[11,29] and that VEGFR signaling which is impaired in DM is involved in P-selectin mobilization from endothelial Weibel-Palade bodies.[10] As a cautionary statement, vasculogenesis in response to fibroblast growth factor-1 in corneal pocket assays is not dependent on selectins,[30] suggesting that selectins are involved in vascular remodeling in response to ischemia but not necessarily in all forms of vascular development.

We assessed P-selectin with CEU which by using a pure intravascular tracer that is able to detect surface translocation of P-selectin in ischemic injury.[31] The higher level of baseline P-selectin expression in skeletal muscle microvessels in the db/db mice is consistent with the notion of chronic upregulation of inflammatory pathways in DM. Yet, db/db mice lacked the ability to mount a substantial P-selectin response after production in ischemia and had a much lower P-selecin signal on molecular imaging at day 1 compared to wild-type mice. Intravital microscopy confirmed a deficit in P-selectin-mediated rolling, although these results must be tempered by the fact that monocytes were not differentiated from other leukocytes. These data are consistent with a notion of a desensitization of the selectin response.

Our studies demonstrated that P-selectin is an important contributor to the vascular response to ischemia and suggest that in db/db mice lower P-selectin response led to less monocyte recruitment and flow recovery in db/db mice. The most compelling evidence is that administration of MCP-1 early after arterial ligation corrected the abnormalities of P-selectin signal on molecular imaging, monocyte infiltration, and flow at day 21 in db/db mice. Within the wild-type group, the early P-selectin signal correlated with the degree of flow recovery at day 21 in animals that were studied at both day 1 and day 21.

There are several limitations of the study that deserve mention. Our data strongly supports but does not positively confirm that abnormal P-selectin response in DM plays a causative role in reduced ischemia-mediated monocyte recruitment and flow recovery. Although the correction of these defects in db/db mice by MCP-1 therapy strongly supports this hypothesis, MCP-1 is a non-specific pro-inflammatory chemokine with many actions. An intervention that specifically acts through selectins would provide stronger evidence but is

currently not available. Although the intravital microscopy data support the concept of a P-selectin defect in db/db mice, it is important to note that the triggers for selectin mobilization may be different for surgical exteriorization versus hindlimb ischemia. Because of surgical technique, we were not able to study every animal at every time interval. Greater P-selectin expression at baseline would seem to argue against our hypothesis. However, there are no data that suggest that the inflammatory response is required for basal vascular homeostasis in non-ischemic conditions. Finally, we also made flow measurements at rest rather than during hyperemia produced by elecrostimulated contractile exercise because of concerns for altering the inflammatory status either through severe ischemia or electrode placement. It is quite likely that the db/db animals would demonstrate an even more profound flow reserve response because of the abnormal NO signaling that occurs as a result of VEGF desensitization.

In summary, we have provided evidence that despite higher basal P-selectin expression in DM, there is reduced expression after inducing chronic limb ischemia consistent with a desensitization of mechanisms that regulate selectin response. The degree of selectin response appears to influence the degree of monocyte recruitment and is also associated with the degree of flow recovery. These data add to our understanding of the mechanisms underlying the impaired response to injury and ischemia in DM and may be helpful in both creating and assessing new strategies aimed at correcting the deficit in the pro-angiogenic inflammatory response.

Supplementary Material

Refer to Web version on PubMed Central for supplementary material.

Acknowledgments

The authors are grateful to Kaitlen Benner and Hillary Johnson for their assistance in analyzing intravital microscopy images.

FUNDING SOURCES

Dr. Lindner is supported by grants R01-HL-078610, R01-DK-063508 and RC1-HL-100659 from the National Institutes of Health. Dr. Carr is supported by a post-doctoral fellowship grant (0820104Z), and Dr. Chadderdon is supported by a Fellow-to-Faculty Transition Award, both from the American Heart Association, Dallas, TX.

References

1. Abaci A, Oguzhan A, Kahraman S, Eryol NK, Unal S, Arinc H, Ergin A. Effect of diabetes mellitus on formation of coronary collateral vessels. Circulation. 1999; 99:2239–2242. [PubMed: 10226087]
2. Yarom R, Zirkin H, Stammler G, Rose AG. Human coronary microvessels in diabetes and ischaemia. Morphometric study of autopsy material. J Pathol. 1992; 166:265–270. [PubMed: 1517882]
3. Martin A, Komada MR, Sane DC. Abnormal angiogenesis in diabetes mellitus. Med Res Rev. 2003; 23:117–145. [PubMed: 12500286]
4. Nahrendorf M, Swirski FK, Aikawa E, Stangenberg L, Wurdinger T, Figueiredo JL, Libby P, Weissleder R, Pittet MJ. The healing myocardium sequentially mobilizes two monocyte subsets with divergent and complementary functions. J Exp Med. 2007; 204:3037–3047. [PubMed: 18025128]
5. Capoccia BJ, Gregory AD, Link DC. Recruitment of the inflammatory subset of monocytes to sites of ischemia induces angiogenesis in a monocyte chemoattractant protein-1-dependent fashion. J Leukoc Biol. 2008; 84:760–768. [PubMed: 18550788]
6. Arras M, Ito WD, Scholz D, Winkler B, Schaper J, Schaper W. Monocyte activation in angiogenesis and collateral growth in the rabbit hindlimb. J Clin Invest. 1998; 101:40–50. [PubMed: 9421464]

7. Waltenberger J, Lange J, Kranz A. Vascular endothelial growth factor-A-induced chemotaxis of monocytes is attenuated in patients with diabetes mellitus: A potential predictor for the individual capacity to develop collaterals. Circulation. 2000; 102:185–190. [PubMed: 10889129]
8. Tchaikovski V, Olieslagers S, Bohmer FD, Waltenberger J. Diabetes mellitus activates signal transduction pathways resulting in vascular endothelial growth factor resistance of human monocytes. Circulation. 2009; 120:150–159. [PubMed: 19564559]
9. Hazarika S, Dokun AO, Li Y, Popel AS, Kontos CD, Annex BH. Impaired angiogenesis after hindlimb ischemia in type 2 diabetes mellitus: differential regulation of vascular endothelial growth factor receptor 1 and soluble vascular endothelial growth factor receptor 1. Circ Res. 2007; 101:948–956. [PubMed: 17823371]
10. Rollin S, Lemieux C, Maliba R, Favier J, Villeneuve LR, Allen BG, Soker S, Bazan NG, Merhi Y, Sirois MG. VEGF-mediated endothelial P-selectin translocation: role of VEGF receptors and endogenous PAF synthesis. Blood. 2004; 103:3789–3797. [PubMed: 14764537]
11. Egami K, Murohara T, Aoki M, Matsuishi T. Ischemia-induced angiogenesis: role of inflammatory response mediated by P-selectin. J Leukoc Biol. 2006; 79:971–976. [PubMed: 16641139]
12. Wan MX, Wang Y, Liu Q, Schramm R, Thorlacius H. CC chemokines induce P-selectin-dependent neutrophil rolling and recruitment in vivo: intermediary role of mast cells. Br J Pharmacol. 2003; 138:698–706. [PubMed: 12598424]
13. Chen H, Charlat O, Tartaglia LA, Woolf EA, Weng X, Ellis SJ, Lakey ND, Culpepper J, Moore KJ, Breitbart RE, Duyk GM, Tepper RI, Morgenstern JP. Evidence that the diabetes gene encodes the leptin receptor: identification of a mutation in the leptin receptor gene in db/db mice. Cell. 1996; 84:491–495. [PubMed: 8608603]
14. Phillips JW, Barringhaus KG, Sanders JM, Hesselbacher SE, Czarnik AC, Manka D, Vestweber D, Ley K, Sarembock IJ. Single injection of P-selectin or P-selectin glycoprotein ligand-1 monoclonal antibody blocks neointima formation after arterial injury in apolipoprotein E-deficient mice. Circulation. 2003; 107:2244–2249. [PubMed: 12707243]
15. Lindner JR, Song J, Christiansen J, Klibanov AL, Xu F, Ley K. Ultrasound assessment of inflammation and renal tissue injury with microbubbles targeted to P-selectin. Circulation. 2001; 104:2107–2112. [PubMed: 11673354]
16. Kaufmann BA, Sanders JM, Davis C, Xie A, Aldred P, Sarembock IJ, Lindner JR. Molecular imaging of inflammation in atherosclerosis with targeted ultrasound detection of vascular cell adhesion molecule-1. Circulation. 2007; 116:276–284. [PubMed: 17592078]
17. Wei K, Jayaweera AR, Firoozan S, Linka A, Skyba DM, Kaul S. Quantification of myocardial blood flow with ultrasound-induced destruction of microbubbles administered as a constant venous infusion. Circulation. 1998; 97:473–483. [PubMed: 9490243]
18. Dawson D, Vincent MA, Barrett EJ, Kaul S, Clark A, Leong-Poi H, Lindner JR. Vascular recruitment in skeletal muscle during exercise and hyperinsulinemia assessed by contrast ultrasound. Am J Physiol Endocrinol Metab. 2002; 282:E714–720. [PubMed: 11832377]
19. Nieswandt B, Bergmeier W, Rackebrandt K, Gessner JE, Zirngibl H. Identification of critical antigen-specific mechanisms in the development of immune thrombocytopenic purpura in mice. Blood. 2000; 96:2520–2527. [PubMed: 11001906]
20. Amin AH, Abd Elmageed ZY, Nair D, Partyka MI, Kadowitz PJ, Belmadani S, Matrougui K. Modified multipotent stromal cells with epidermal growth factor restore vasculogenesis and blood flow in ischemic hind-limb of type II diabetic mice. Lab Invest. 90:985–996. [PubMed: 20440273]
21. Li Y, Hazarika S, Xie D, Pippen AM, Kontos CD, Annex BH. In mice with type 2 diabetes, a vascular endothelial growth factor (VEGF)-activating transcription factor modulates VEGF signaling and induces therapeutic angiogenesis after hindlimb ischemia. Diabetes. 2007; 56:656–665. [PubMed: 17327433]
22. Emanueli C, Caporali A, Krankel N, Cristofaro B, Van Linthout S, Madeddu P. Type-2 diabetic Lepr(db/db) mice show a defective microvascular phenotype under basal conditions and an impaired response to angiogenesis gene therapy in the setting of limb ischemia. Front Biosci. 2007; 12:2003–2012. [PubMed: 17127438]

23. Yan J, Tie G, Park B, Yan Y, Nowicki PT, Messina LM. Recovery from hind limb ischemia is less effective in type 2 than in type 1 diabetic mice: roles of endothelial nitric oxide synthase and endothelial progenitor cells. J Vasc Surg. 2009; 50:1412–1422. [PubMed: 19837544]
24. Clerk LH, Vincent MA, Barrett EJ, Lankford MF, Lindner JR. Skeletal muscle capillary responses to insulin are abnormal in late-stage diabetes and are restored by angiotensin-converting enzyme inhibition. Am J Physiol Endocrinol Metab. 2007; 293:E1804–1809. [PubMed: 17911341]
25. Jayaweera AR, Wei K, Coggins M, Bin JP, Goodman C, Kaul S. Role of capillaries in determining CBF reserve: new insights using myocardial contrast echocardiography. Am J Physiol. 1999; 277:H2363–2372. [PubMed: 10600857]
26. Ito WD, Arras M, Winkler B, Scholz D, Schaper J, Schaper W. Monocyte chemotactic protein-1 increases collateral and peripheral conductance after femoral artery occlusion. Circ Res. 1997; 80:829–837. [PubMed: 9168785]
27. Heil M, Ziegelhoeffer T, Wagner S, Fernandez B, Helisch A, Martin S, Tribulova S, Kuziel WA, Bachmann G, Schaper W. Collateral artery growth (arteriogenesis) after experimental arterial occlusion is impaired in mice lacking CC-chemokine receptor-2. Circ Res. 2004; 94:671–677. [PubMed: 14963007]
28. Voskuil M, Hoefer IE, van Royen N, Hua J, de Graaf S, Bode C, Buschmann IR, Piek JJ. Abnormal monocyte recruitment and collateral artery formation in monocyte chemoattractant protein-1 deficient mice. Vasc Med. 2004; 9:287–292. [PubMed: 15678621]
29. Yukami T, Hasegawa M, Matsushita Y, Fujita T, Matsushita T, Horikawa M, Komura K, Yanaba K, Hamaguchi Y, Nagaoka T, Ogawa F, Fujimoto M, Steeber DA, Tedder TF, Takehara K, Sato S. Endothelial selectins regulate skin wound healing in cooperation with L-selectin and ICAM-1. J Leukoc Biol. 2007; 82:519–531. [PubMed: 17595378]
30. Hartwell DW, Butterfield CE, Frenette PS, Kenyon BM, Hynes RO, Folkman J, Wagner DD. Angiogenesis in P- and E-selectin-deficient mice. Microcirculation. 1998; 5:173–178. [PubMed: 9789257]
31. Kaufmann BA, Lewis C, Xie A, Mirza-Mohd A, Lindner JR. Detection of recent myocardial ischaemia by molecular imaging of P-selectin with targeted contrast echocardiography. Eur Heart J. 2007; 28:2011–2017. [PubMed: 17526905]

APPENDIX

Acoustic intensity (I_p) due to microbubles transiting through a tissue bed at time t is given by

$$I_p = k \cdot C_t \cdot v \tag{1}$$

where C_t is the concentration of microbubles in blood at time t, v is the blood volume fraction and k is a proportionality constant. The amount of microbubbles dW that passes through a unit volume of tissue over a time interval dt at time t is given by

$$dW = F \cdot C_t \cdot dt \tag{2}$$

where F is the blood flow per unit volume of tissue. Therefore, the total amount of microbubbles W that passes through tissue over a time interval t is

$$W = F \cdot \int_0^t C_t \cdot dt \tag{3}$$

If a fraction *f* of these bubbles is retained by tissue, the acoustic intensity that is attributable to these retained bubbles (I_r) is

$$I_r = k \cdot f \cdot W \tag{4}$$

Hence the total intensity at time *t* (I_t) is given by

$$I_T = I_p + I_r = k \cdot [C_t \cdot v + f \cdot W] = k \cdot [C_t \cdot v + f \cdot F \cdot \int_0^t C_t \cdot dt] \tag{5}$$

From perfusion imaging data, we know that $v = A_n$, where A_n is plateau video intensity normalized to blood pool intensity and $F = A_n.\beta$, where β is the rate constant from the post-destructive CEU data. Also, we know that

$$C_t = A \cdot t \cdot e^{-\alpha t} \tag{6}$$

and also that

$$\int_0^t C_t \cdot dt = (A/\alpha^2) \cdot [1 - (1+\alpha \cdot t)\, e^{-\alpha t}] \tag{7}$$

Substituting equations 6 and 7 in equation 5 and simplifying we get

$$I_T = (K \cdot A_n \cdot A) \cdot [t \cdot e^{-\alpha t} + (f \cdot \beta/\alpha^2) \cdot \{1 - (1+\alpha t) \cdot e^{-\alpha t}\}] \tag{8}$$

Hence, the retention fraction *f* can be obtained by substituting the known value of β and fitting equation 8 to time versus intensity data obtained after injection of the targeted tracer.

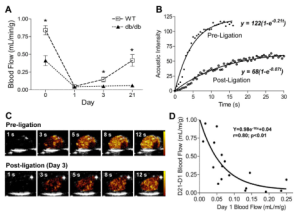

Figure 1.

Skeletal muscle blood flow by CEU. (**A**) Skeletal muscle blood flow at baseline (day 0) and at subsequent days after arterial ligation. *p<0.05 vs db/db. See online supplement for number of observations for each data point. (**B and C**) Examples of time-intensity data from the proximal hindlimb adductor muscle group after a destructive high-power ultrasound pulse sequence prior to ligation and at post-ligation day 3, and corresponding background-subtracted color-coded CEU images (scale at right). (**D**) Relation between muscle blood flow on day 1 (initial degree of ischemia) and subsequent change in blood flow between day 1 and 21.

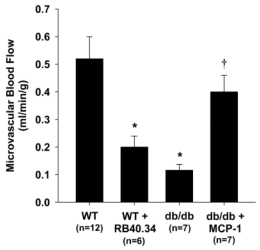

Figure 2.

Mean (±SEM) skeletal muscle blood flow at day 21 after arterial ligation in wild-type with and without P-selectin blocking antibody RB40.34, and db/db mice with and without MCP-1 treatment. *p<0.01 vs wild-type; †p<0.05 vs untreated db/db mice.

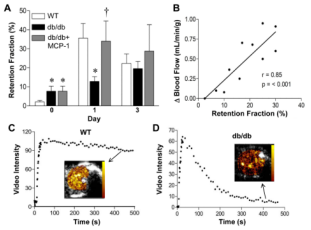

Figure 3.

Targeted CEU molecular imaging of P-selectin. (**A**) Retention fraction for P-selectin targeted microbubbles prior to (day 0) and at days 1 and 3 after arterial ligation. Baseline data for MCP-1-treated and untreated db/db mice are identical since these represent combined pre-treatment data. *p<0.01 vs wild-type; †p<0.05 vs untreated db/db mice. See online supplement for number of observations for each data point. (**B**) Relation between retention fraction of P-selectin microbubbles on day 1 and subsequent change in blood flow between day 1 and 21. (**C and D**) Examples of time-intensity data from the proximal hindlimb adductor muscle after intravenous injection of P-selectin-targeted microbubbles illustrating differences in muscle retention fraction from a wild-type and db/db mouse one day after arterial ligation. Examples of backround-subtracted video color-coded (scale at left) video intensity near the end of the acquisition are illustrated.

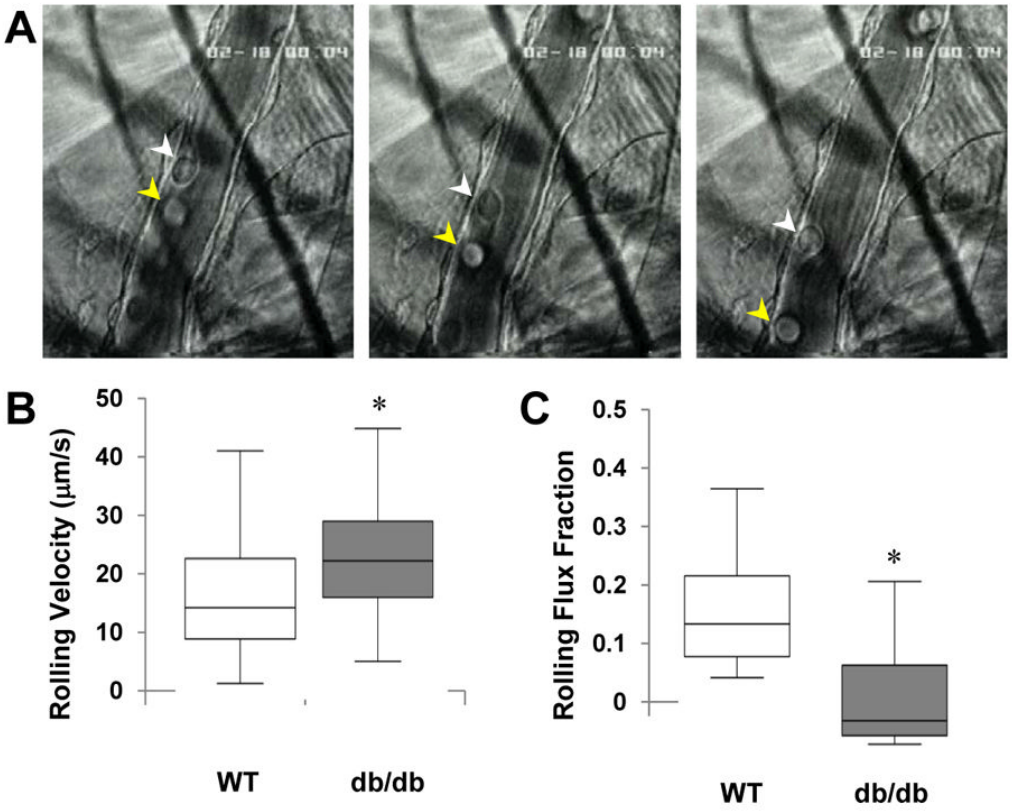

Figure 4.

Intravital microscopy of leukocyte rolling. (**A**) Selected images 0.3 s apart from a video illustrating two separate leukocytes (white and yellow arrowheads) rolling on the endothelial surface of a 25 μm diameter venule. Bar-whisker plots displaying median (line), 25–75% percentile (box), and range for (**B**) leukocyte rolling velocity and (**C**) leukocyte flux fraction. *p<0.01 vs wild-type.

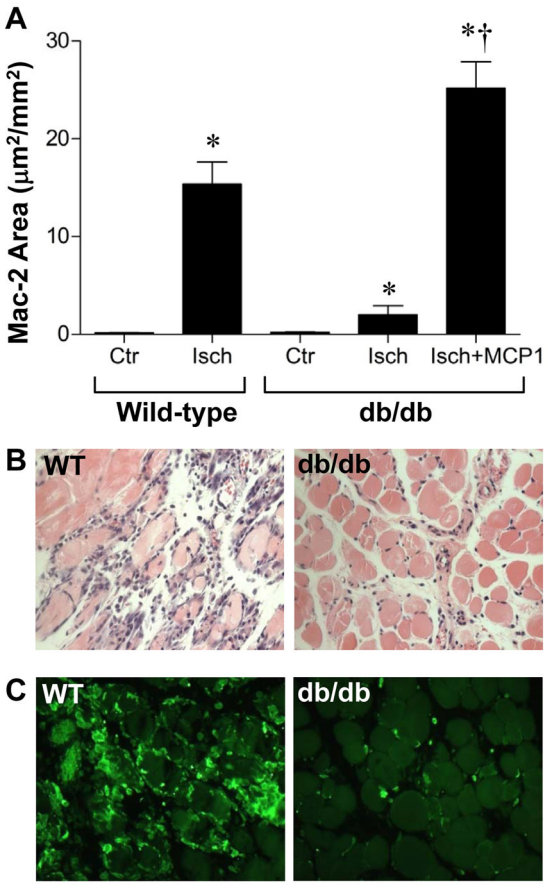

Figure 5.

Inflammation on muscle histology. (**A**) Area staining positive for Mac-2 on day 3 after ischemia expressed as a percentage of total area. Data are shown for the ischemic and contralateral control hindlimb. *p<0.01 vs control leg; †p<0.01 vs untreated db/db mice. Examples of (**B**) hematoxylin & eosin staining, and (**C**) Mac-2 immunohistochemistry from the ischemic limb of a wild-type and db/db mouse at day 3 after arterial ligation.